



On the Inflation of Residually Stressed Spherical Shells

Atacan Yucesoy¹ · Thomas J. Pence¹

Dedicated to M. F. Beatty on the occasion of his 90th birthday.

Received: 5 May 2021 / Accepted: 24 October 2021 / Published online: 30 November 2021
© The Author(s), under exclusive licence to Springer Nature B.V. 2021

Abstract

A well known result from the non-linear theory of elasticity applied to spherical shells is that the classical Mooney-Rivlin constitutive law may give either a monotonic or a non-monotonic pressure-inflation response for finite deformation. Specifically, this is determined by two factors: the relative shell thickness, and the relative I_1 to I_2 contribution in the M-R constitutive law. Here we consider how a residual stress field may affect this behavior. Using a constitutive framework for hyperelastic materials with residual stress that has been especially applied to tubes, this paper focuses on finite thickness spherical shells while using a similar prototypical energy response. In this context we examine different residual stress states, and show how certain of these lead to more workable analytical results than others. All of them enable Taylor and asymptotic expansions in the small and large inflation limit. On this basis it is shown how particular residual stress fields can cause a monotonic inflation graph to become non-monotonic, and vice versa.

Keywords Residual stress · Non-linear elasticity · Thick spherical shell · Finite deformation · Non-monotone inflation

Mathematics Subject Classification 74B20

1 Introduction

Spherically symmetric deformation is a classical topic in continuum mechanics. For incompressible materials, the symmetric inflation of a spherical shell is completely characterized by the displacement of a single location. If the material is also isotropic and hyperelastic, then this inflation deformation is controllable, meaning equilibrium is obtainable by the application of surface tractions alone (in this case a pressure difference between the inner and outer radii). Because this “controllable deformation can be effected in every homogeneous, isotropic, hyperelastic material [it] is ... a universal deformation”. This quote is from Beatty’s

✉ T.J. Pence
pence@egr.msu.edu

A. Yucesoy
yucesoya@msu.edu

¹ Michigan State University, East Lansing, MI, USA

1996 *Introduction to Nonlinear Elasticity* [3]. This work describes spherical inflation in detail, in addition to discussing universal deformations and their relation to Ericksen's problem of characterizing the full set of universal deformations. Elsewhere, Beatty describes how the incompressible hyperelastic spherical shell admits to interesting and elegant fully dynamical analysis for the case of small amplitude radial oscillations [4].

Returning to the equilibrium setting, one of the notable aspects of the inflation problem for a spherical shell is that the well known and often used Mooney-Rivlin (MR) hyperelastic model permits a nonmonotonic pressure-inflation response. Whether the response of a given MR spherical shell is monotonic or nonmonotonic is determined by the key MR constitutive parameter in conjunction with the shell initial geometry (typically taken to be the wall thickness as compared to the initial inner radius). Nonmonotonicity of the inflation response has immediate consequences for the stability of any ongoing inflation process (again [3], and see [18] for detailed thermodynamic considerations). It is also connected to loss-of-symmetry via bifurcation to pear-shaped axisymmetric states [6, 12]. The consideration of additional driving fields, such as that associated with electrical actuation, lead to rich possibilities for such pear-shaped bifurcated states, which in general lower the total energy [25].

In this work we consider some effects of residual stress on spherically symmetric deformation in such pressurized spherical shells. The conception of residual stress follows that of Hoger [13, 14]. The specific hyperelastic framework employed here follows the invariant formulation presented in [24]. That formulation is further developed and utilized in subsequent treatments for residual stress including [10, 17] and [23]. These and other recent contributions are discussed at relevant points in this article. Because of the important connection to residual stress in blood vessels, several of these articles consider tube-type situations and hence boundary value problems posed in cylindrical coordinates.

In general, biological growth and remodeling leads to residual stress, a process that is examined for spherical shells in [7] and [9]. A related phenomenon for spherical shells is the effect of inhomogeneous wall swelling on a hyperelastic pressure-inflation relation [27], including how this compares to the baseline response with uniform wall swelling [26]. An examination of symmetry breaking bifurcations that may cause deformation in a residually stressed solid sphere to depart from spherical symmetry is given in [20].

The present article is organized as follows. The general residual stress conception and its hyperelastic constitutive formulation is given in Sect. 2, followed by the specialization to spherically symmetric deformations in Sect. 3. Classes of spherically symmetric residual stress fields are introduced in Sect. 4. The integration procedure for the solution of the boundary value problem is given in Sect. 5. This leads to the consideration of specific integrals associated with the residual stress field, whose properties are examined in Sect. 6. This property determination permits a rather straight forward assessment of how the residual stress affects the pressure-inflation relation. Among the findings of interest is that particular residual stress fields can cause a monotonic inflation graph to become non-monotonic, and vice versa. Key limitations of our study are discussed in Sect. 8, some of which are associated with the elusive nature of the meaning of residual stress, along with an indication of how some of the analytical findings here could be further exploited.

2 Residual Stress Framework and Constitutive Modeling

We consider a body that inhabits locations \mathbf{X} in a reference configuration \mathcal{B}_0 . A residual stress is present within the body in this reference configuration, where it is given by the tensor $\boldsymbol{\tau}$. The reason for the existence of the residual stress is not important – the nature

of the theory permits the consideration of residual stress fields independent of their cause. Whatever this cause, the residual stress field is subject to the classical balance of torques and forces in the usual way. Intrinsic couple stresses are not considered whereupon the torque balance gives that $\boldsymbol{\tau}$ is symmetric ($\boldsymbol{\tau}^T = \boldsymbol{\tau}$). Body forces are regarded as negligible, whereupon force balance gives that

$$\text{Div } \boldsymbol{\tau} = \mathbf{0}, \quad (2.1)$$

where Div is the divergence operation with respect to reference locations \mathbf{X} . The residual stress is present in the absence of surface tractions, meaning that

$$\boldsymbol{\tau} \mathbf{N} = \mathbf{0} \quad \text{on } \partial \mathcal{B}_0, \quad (2.2)$$

where $\partial \mathcal{B}_0$ is the external boundary of \mathcal{B}_0 and \mathbf{N} the outward pointing unit normal vector. This follows the residual stress conception of Hoger [13]. Other notions of initial stress may incorporate sustaining surface tractions, whereas none are to be present here. A consequence of conditions (2.1) and (2.2) is that the mean value of the residual stress over \mathcal{B}_0 must vanish [14], namely

$$\int_{\mathcal{B}_0} \boldsymbol{\tau} dV = \mathbf{0}. \quad (2.3)$$

For this reason, any nontrivial $\boldsymbol{\tau}$ will generally cause an inhomogeneous mechanical response to subsequent deformation.

The application of surface tractions will deform the body to a new configuration \mathcal{B} . Let \mathbf{x} denote locations in \mathcal{B} . The deformation gradient of the mapping $\mathbf{X} \rightarrow \mathbf{x}$ is denoted by \mathbf{F} in the usual way. This process will generally change the internal stress field so that it is no longer given by $\boldsymbol{\tau}$. Let $\boldsymbol{\sigma}$ denote the associated Cauchy stress tensor. If $\mathbf{F} = \mathbf{I}$ then $\boldsymbol{\sigma}$ is equal to $\boldsymbol{\tau}$ modulo a purely reactive stress contribution associated with any internal material constraints (such as incompressibility). The Cauchy stress is also symmetric and it is subject to

$$\text{div } \boldsymbol{\sigma} = \mathbf{0}, \quad (2.4)$$

where div is the divergence operation with respect to deformed locations \mathbf{x} . The surface tractions \mathbf{t} follow from $\boldsymbol{\sigma}$ and the unit surface normal \mathbf{n} on $\partial \mathcal{B}$ via

$$\mathbf{t} = \boldsymbol{\sigma} \mathbf{n} \quad \text{on } \partial \mathcal{B}. \quad (2.5)$$

A hyperelastic constitutive framework is employed here which follows that described in [24]. It is given in terms of a stored energy density function $W = W(\mathbf{C}, \boldsymbol{\tau})$ where $\mathbf{C} = \mathbf{F}^T \mathbf{F}$ is the usual right Cauchy-Green deformation tensor. This form ensures the axiom of objectivity. One could more generally allow an explicit inhomogeneous response $W = W(\mathbf{C}, \boldsymbol{\tau}, \mathbf{X})$ but this more general case is not considered here. It is important to note that the spatial dependence $\boldsymbol{\tau} = \boldsymbol{\tau}(\mathbf{X})$ confers the implicit inhomogeneous response (mentioned above) even in the context of the $W = W(\mathbf{C}, \boldsymbol{\tau})$ treatment.

Attention is here restricted to incompressible materials, meaning that deformations $\mathbf{X} \rightarrow \mathbf{x}$ must be volume preserving. This gives the standard isochoric constraint

$$\det \mathbf{F} = 1. \quad (2.6)$$

The Cauchy stress now follows from \mathbf{F} via

$$\boldsymbol{\sigma} = \mathbf{F} \frac{\partial W}{\partial \mathbf{C}} \mathbf{F}^T - p \mathbf{I}, \tag{2.7}$$

where p is the non-constitutive reactive pressure associated with (2.6). Because $\mathbf{F} = \mathbf{I}$ implies $\boldsymbol{\sigma} = \boldsymbol{\tau}$ to within a hydrostatic pressure it follows that

$$\boldsymbol{\tau} = \left. \frac{\partial W}{\partial \mathbf{C}} \right|_{\mathbf{C}=\mathbf{I}} - q \mathbf{I}, \tag{2.8}$$

for some scalar q and, as discussed in [24], this imposes restrictions upon W .

Still following [24], the dependence of W upon \mathbf{C} and $\boldsymbol{\tau}$ can be developed in terms of a set of nine independent invariants of \mathbf{C} , $\boldsymbol{\tau}$ and their combination. These can be taken as the two usual isochoric invariants of \mathbf{C} alone:

$$I_1 = \text{tr} \mathbf{C}, \quad I_2 = \frac{1}{2} [(\text{tr} \mathbf{C})^2 - \text{tr}(\mathbf{C}^2)]; \tag{2.9}$$

(note that $I_3 = \det \mathbf{C} = 1$), the three invariants of $\boldsymbol{\tau}$ alone:

$$I_{41} = \text{tr} \boldsymbol{\tau}, \quad I_{42} = \frac{1}{2} [(\text{tr} \boldsymbol{\tau})^2 - \text{tr}(\boldsymbol{\tau}^2)], \quad I_{43} = \det \boldsymbol{\tau}; \tag{2.10}$$

and four independent invariants of both \mathbf{C} and $\boldsymbol{\tau}$ in combination:

$$I_5 = \text{tr}(\boldsymbol{\tau} \mathbf{C}), \quad I_6 = \text{tr}(\boldsymbol{\tau} \mathbf{C}^2), \quad I_7 = \text{tr}(\boldsymbol{\tau}^2 \mathbf{C}), \quad I_8 = \text{tr}(\boldsymbol{\tau}^2 \mathbf{C}^2). \tag{2.11}$$

Here we consider the specific invariant sets employed in [16]. The three invariants $\{I_{41}, I_{42}, I_{43}\}$ are collectively denoted by I_4 . They are singled out this way because, unlike the other invariants, they do not contribute derivatives to $\boldsymbol{\sigma}$ via (2.7) by a chain rule calculation on $\partial W / \partial \mathbf{C}$. Letting $W_i = \partial W / \partial I_i$ for $i = 1, 2, 5, 6, 7, 8$ such a chain rule calculation gives

$$\begin{aligned} \boldsymbol{\sigma} = & 2W_1 \mathbf{B} + 2W_2 (I_1 \mathbf{B} - \mathbf{B}^2) + 2W_5 \boldsymbol{\Sigma} + 2W_6 (\boldsymbol{\Sigma} \mathbf{B} + \mathbf{B} \boldsymbol{\Sigma}) \\ & + 2W_7 \boldsymbol{\Sigma} \mathbf{B}^{-1} \boldsymbol{\Sigma} + 2W_8 (\boldsymbol{\Sigma} \mathbf{B}^{-1} \boldsymbol{\Sigma} \mathbf{B} + \mathbf{B} \boldsymbol{\Sigma} \mathbf{B}^{-1} \boldsymbol{\Sigma}) - p \mathbf{I}, \end{aligned} \tag{2.12}$$

where, following [16], $\boldsymbol{\Sigma} \equiv \mathbf{F} \boldsymbol{\tau} \mathbf{F}^T$, and $\mathbf{B} = \mathbf{F} \mathbf{F}^T$ is the left Cauchy-Green tensor. Note that (2.12) retrieves the classical (no-residual-stress) hyperelastic result $\boldsymbol{\sigma} = 2W_1 \mathbf{B} + 2W_2 (I_1 \mathbf{B} - \mathbf{B}^2) - p \mathbf{I}$ when $\boldsymbol{\tau}$ vanishes.

A simple model form for W to consider is one that admits the decomposition $W = W_o(I_1, I_2) + W_\tau(I_5, I_6, I_7, I_8)$. By taking W_o to be some well vetted hyperelastic model from the conventional isotropic theory, it permits a consideration of the effect of residual stress upon standard results. Forms for W_τ that have received consideration (see [16]) include

$$W_\tau = \frac{1}{2} (I_5 - \text{tr}(\boldsymbol{\tau})) \quad \text{and} \quad W_\tau = \frac{1}{4} (I_6 - \text{tr}(\boldsymbol{\tau})). \tag{2.13}$$

Note that $I_5, I_6, \text{tr}(\boldsymbol{\tau})$ and W_τ all have the same physical units, so that $\frac{1}{2}$ and $\frac{1}{4}$ in (2.13) are pure numbers. The particular values $\frac{1}{2}$ and $\frac{1}{4}$ in (2.13) are essential as they enable consistency with (2.8).

In what follows we shall consider a Mooney-Rivlin form for W_o , namely

$$W_o = \frac{1}{2} \mu (\kappa (I_1 - 3) + (1 - \kappa) (I_2 - 3)). \tag{2.14}$$

Here μ , with units of stress, is the shear modulus. The pure number κ is taken to be in the range $0 \leq \kappa \leq 1$ in order for the conventional theory to be consistent with the Baker-Ericksen inequalities. The value $\kappa = 1$ gives the neo-Hookean special case. Values for κ a bit below one are often regarded as providing a suitable first correction to the neo-Hookean theory [21].

Expressing $W = W_o + W_\tau$ by combining (2.14) with the first of (2.13) gives

$$W = \frac{1}{2}\mu (\kappa(I_1 - 3) + (1 - \kappa)(I_2 - 3)) + \frac{1}{2}(I_5 - \text{tr}(\boldsymbol{\tau})). \quad (2.15)$$

This form for W , under the neo-Hookean specialization ($\kappa = 1$), has been utilized for the analysis of residually stressed cylinders in [17] and [16]. Also, the neo-Hookean case of (2.15) where W_τ is allowed to be augmented with a quadratic term proportional to $(I_5 - \text{tr}(\boldsymbol{\tau}))^2$ has been considered for the examination of acoustic waves [24] and Rayleigh waves [23] in residually stressed materials. Restricting attention to (2.15) it now follows from (2.12) that

$$\boldsymbol{\sigma} = \mu ((\kappa + (1 - \kappa)I_1)\mathbf{B} - (1 - \kappa)\mathbf{B}^2) + \mathbf{F}\boldsymbol{\tau}\mathbf{F}^T - p\mathbf{I}, \quad (2.16)$$

where it is observed that $\mathbf{F} = \mathbf{I}$ and $p = (2 - \kappa)\mu$ indeed makes $\boldsymbol{\sigma} = \boldsymbol{\tau}$.

3 Kinematics for Radial Inflation of a Residually-Stressed Spherical Shell

We consider a finite thickness spherical shell that, using spherical coordinates (R, Θ, Φ) , occupies

$$A \leq R \leq B, \quad 0 \leq \Theta < \pi, \quad 0 \leq \Phi \leq \pi \quad (3.1)$$

in the reference configuration \mathcal{B}_0 . Here A and B are inner and outer radii prior to any deformation. Spherical inflation, which is one of the universal deformations in the conventional isotropic, incompressible hyperelastic theory, is then described using spherical coordinates (r, θ, ϕ) in the deformed configuration \mathcal{B} , as

$$r = r(R), \quad \theta = \Theta, \quad \phi = \Phi. \quad (3.2)$$

The deformation gradient is given by

$$\mathbf{F} = \lambda_r \mathbf{e}_r \otimes \mathbf{E}_R + \lambda_\theta \mathbf{e}_\theta \otimes \mathbf{E}_\Theta + \lambda_\phi \mathbf{e}_\phi \otimes \mathbf{E}_\Phi, \quad (3.3)$$

where $\{\mathbf{E}_R, \mathbf{E}_\Theta, \mathbf{E}_\Phi\}$ and $\{\mathbf{e}_r, \mathbf{e}_\theta, \mathbf{e}_\phi\}$ are the unit basis vectors in the reference and deformed configuration respectively, and

$$\lambda_r = \frac{dr}{dR}, \quad \lambda_\theta = \lambda_\phi = \frac{r}{R} \quad (3.4)$$

are the principal stretches in the corresponding directions. The associated right and left Cauchy-Green deformation tensors are

$$\begin{aligned} \mathbf{C} &= \lambda_r^2 \mathbf{E}_R \otimes \mathbf{E}_R + \lambda_\theta^2 (\mathbf{E}_\Theta \otimes \mathbf{E}_\Theta + \mathbf{E}_\Phi \otimes \mathbf{E}_\Phi), \\ \mathbf{B} &= \lambda_r^2 \mathbf{e}_r \otimes \mathbf{e}_r + \lambda_\theta^2 (\mathbf{e}_\theta \otimes \mathbf{e}_\theta + \mathbf{e}_\phi \otimes \mathbf{e}_\phi). \end{aligned} \quad (3.5)$$

The constraint (2.6) determines $r(R)$ to within a single constant parameter value, which can be taken as the radial value a of the deformed inner radius. Then

$$r(R) = (R^3 - A^3 + a^3)^{1/3}, \tag{3.6}$$

whereupon the deformed sphere occupies $a \leq r \leq b = (B^3 - A^3 + a^3)^{1/3}$. Consequently the relation between A and a completely characterizes the amount of inflation. This also makes it convenient to emphasize the azimuthal stretch via the notation

$$\lambda \equiv \lambda_\theta = \lambda_\phi = \frac{r}{R} \quad \Rightarrow \quad \lambda_r = \lambda^{-2} = \frac{R^2}{r^2}. \tag{3.7}$$

The reference configuration is subject to the no surface traction condition (2.2), and the inflation is induced by increasing the internal pressure by an amount $\Delta P > 0$. Such loading is consistent with a radial deformation (3.2) in the conventional theory where there is no residual stress. In order to remain consistent with spherical inflation, consider residual stress fields of the symmetric form $\boldsymbol{\tau} = \tau_{RR}\mathbf{E}_R \otimes \mathbf{E}_R + \tau_{\Theta\Theta}(\mathbf{E}_\Theta \otimes \mathbf{E}_\Theta + \mathbf{E}_\Phi \otimes \mathbf{E}_\Phi)$ with $\tau_{RR} = \tau_{RR}(R)$ and $\tau_{\Theta\Theta} = \tau_{\Theta\Theta}(R)$. Then (2.1) and (2.2) respectively give

$$\frac{d\tau_{RR}}{dR} + \frac{2}{R}(\tau_{RR} - \tau_{\Theta\Theta}) = 0, \tag{3.8}$$

and

$$\tau_{RR}(A) = 0, \quad \tau_{RR}(B) = 0. \tag{3.9}$$

A general result that follows from (3.8) and (3.9) is that

$$\int_A^B ((m - 1)\tau_{RR} + 2\tau_{\Theta\Theta})R^m dR = 0, \tag{3.10}$$

where m is arbitrary. The cases $m = 1$ and $m = 2$ then give

$$\int_A^B \tau_{\Theta\Theta} R dR = 0, \quad \int_A^B (\tau_{RR} + 2\tau_{\Theta\Theta})R^2 dR = 0. \tag{3.11}$$

The first of these establishes that a nontrivial $\tau_{\theta\theta}$ field must take on both tensile and compressive values. The second of these is what (2.3) reduces to for the problem under consideration here.

The Cauchy stress $\boldsymbol{\sigma}$ takes the form $\boldsymbol{\sigma} = \sigma_{rr}\mathbf{e}_r \otimes \mathbf{e}_r + \sigma_{\theta\theta}(\mathbf{e}_\theta \otimes \mathbf{e}_\theta + \mathbf{e}_\phi \otimes \mathbf{e}_\phi)$ with $\sigma_{rr} = \sigma_{rr}(r)$ and $\sigma_{\theta\theta} = \sigma_{\theta\theta}(r)$. In particular, it follows from (2.16), (3.3) and (3.7) that

$$\sigma_{rr} = \mu (2(1 - \kappa)\lambda^{-2} + \kappa\lambda^{-4}) + \lambda^{-4}\tau_{RR} - p, \tag{3.12}$$

and

$$\sigma_{\theta\theta} = \mu ((1 - \kappa)\lambda^4 + \kappa\lambda^2 + (1 - \kappa)\lambda^{-2}) + \lambda^2\tau_{\Theta\Theta} - p. \tag{3.13}$$

The equilibrium equation (2.4) gives $p = p(r)$ along with the one nontrivial requirement

$$\frac{\partial\sigma_{rr}}{\partial r} + \frac{2}{r}(\sigma_{rr} - \sigma_{\theta\theta}) = 0. \tag{3.14}$$

In terms of the applied pressures, the surface traction condition (2.5) is simply

$$\sigma_{rr}(a) = -\Delta P, \quad \sigma_{rr}(b) = 0. \tag{3.15}$$

4 The Residual Stress Fields

Given a τ_{RR} field, the associated $\tau_{\Theta\Theta}$ follows from (3.8). Probably the simplest nontrivial τ_{RR} field that is consistent with (3.9) is a parabolic profile proportional to $(R - A)(R - B)$. We write this as

$$\tau_{RR}(R) = \frac{\alpha_2}{A^2}(R - A)(R - B) = \frac{\alpha_2}{A^2}(R^2 - (A + B)R + AB) \quad (4.1)$$

where α_2 , with units of stress, sets the field strength. The analogous radial component field was considered in [16] for the case of a cylindrical geometry. For the spherical geometry under consideration here, using (3.8) with the τ_{RR} field given by (4.1) yields

$$\tau_{\Theta\Theta}(R) = \frac{\alpha_2}{A^2} \left(2R^2 - \frac{3}{2}(A + B)R + AB \right). \quad (4.2)$$

The subscript 2 in α_2 is indicative of the highest power of R in these expressions.

We wish to consider a wider variety of residual stress fields ($\tau_{RR}(R)$, $\tau_{\Theta\Theta}(R)$) beyond that given by (4.1) and (4.2). For reasons that will become clear later, it will also be advantageous to consider τ_{RR} fields that consist of a linear combination of terms in R^0 , R^2 , R^5 , and more generally R^{2+n} for $n = 0, 1, 2, \dots$. Then the boundary conditions (3.9) motivates the consideration of

$$\tau_{RR}(R) = \frac{\alpha_5}{A^5} \left(R^5 - \left(\frac{B^5 - A^5}{B^2 - A^2} \right) R^2 + \frac{A^2 B^2 (B^3 - A^3)}{B^2 - A^2} \right), \quad (4.3)$$

as well as higher order forms such as

$$\tau_{RR}(R) = \frac{\alpha_8}{A^8} \left(R^8 - \left(\frac{B^8 - A^8}{B^5 - A^5} \right) R^5 + \frac{A^5 B^5 (B^3 - A^3)}{B^5 - A^5} \right), \quad (4.4)$$

and

$$\tau_{RR}(R) = \frac{\alpha_{11}}{A^{11}} \left(R^{11} - \left(\frac{B^{11} - A^{11}}{B^8 - A^8} \right) R^8 + \frac{A^8 B^8 (B^3 - A^3)}{B^8 - A^8} \right). \quad (4.5)$$

The multiplier coefficients $\alpha_2, \alpha_5, \alpha_8, \alpha_{11}$ in (4.1)-(4.5), all with units of stress, will serve as a useful marker for distinguishing between these different fields in the various examples that follow.

The $\tau_{\Theta\Theta}$ corresponding to (4.3)-(4.5) will again follow from (3.8). In making such a computation, and especially for later developments, it is useful to proceed term by term in the residual stress expressions such as (4.3). We will utilize the overbar notation $\bar{\tau}$ for this purpose. Thus employing (3.8) gives the single term result

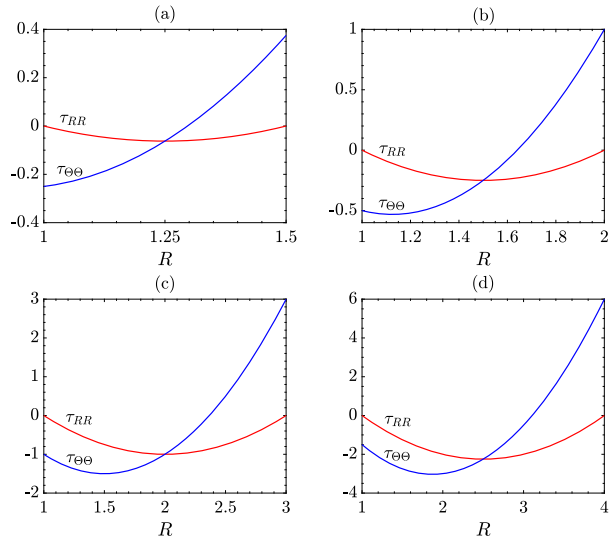
$$\bar{\tau}_{RR} = c R^q, \quad \Rightarrow \quad \bar{\tau}_{\Theta\Theta} = c \left(1 + \frac{1}{2}q \right) R^q. \quad (4.6)$$

Consequently, if τ_{RR} is given by (4.3) then

$$\tau_{\Theta\Theta}(R) = \frac{\alpha_5}{A^5} \left(\frac{7}{2} R^5 - 2 \left(\frac{B^5 - A^5}{B^2 - A^2} \right) R^2 + \frac{A^2 B^2 (B^3 - A^3)}{B^2 - A^2} \right). \quad (4.7)$$

The purpose of the $\bar{\tau}$ notation is to provide a reminder that a single term within the overall multi-term expression is unlikely to be consistent with (3.9). Thus (4.7) is consistent with (3.9) whereas (4.6) is not. Rather, (4.6) is a preliminary single term result that will be used

Fig. 1 Residual stress fields (4.1) for τ_{RR} (red) and (4.2) for $\tau_{\Theta\Theta}$ (blue) showing the effect of shell thickness. Here $\alpha_2 = 1, A = 1$ and: (a) $B=1.5$, (b) $B=2$, (c) $B=3$, and (d) $B=4$



in conjunction with other single term expressions to achieve consistency with the boundary conditions.

For completeness in what follows, the $\tau_{\Theta\Theta}$ field associated with (4.4) now also follows as

$$\tau_{\Theta\Theta}(R) = \frac{\alpha_8}{A^8} \left(5R^8 - \frac{7}{2} \left(\frac{B^8 - A^8}{B^5 - A^5} \right) R^5 + \frac{A^5 B^5 (B^3 - A^3)}{B^5 - A^5} \right), \tag{4.8}$$

and the $\tau_{\Theta\Theta}$ field associated with (4.5) follows as

$$\tau_{\Theta\Theta}(R) = \frac{\alpha_{11}}{A^{11}} \left(\frac{13}{2} R^{11} - 5 \left(\frac{B^{11} - A^{11}}{B^8 - A^8} \right) R^8 + \frac{A^8 B^8 (B^3 - A^3)}{B^8 - A^8} \right). \tag{4.9}$$

Figure 1 shows the effect of thickness on the residual stress field pair given by (4.1) and (4.2). The 2-D counterpart to this figure is Fig. 1 of [16]. As in the 2-D case, the $\tau_{\Theta\Theta}$ fields transition from monotone to non-monotone as the thickness increases. The minimum develops sooner in the present 3-D case since, unlike the 2-D case, it is readily apparent here for the case of $A = 1, B = 2$. Note also the qualitative similarity of these fields, which are independent of constitutive law, to the residual stress field displayed in Fig. 3 of [15] that is associated with the eversion of a spherical shell composed of a particular Mooney-Rivlin material.

For a common shell thickness, Fig. 2 displays the four different stress field pairs ($\tau_{RR}, \tau_{\Theta\Theta}$) as τ_{RR} is given by the four alternatives: (4.1), (4.3), (4.4) and (4.5). In particular, τ_{RR} is of a single sign in all four cases. In contrast, $\tau_{\Theta\Theta}$ takes on both positive and negative values, a result which follows from the first of (3.11). Note also that the fields increasingly localize to the outer radius $R = B$ as the order (highest power of R) increases in the residual stress fields. This tendency is highlighted in Fig. 3 which redisplayes the stress fields from Fig. 2, but now with α_i chosen so that $\tau_{\Theta\Theta}(B) = 1$ for all four alternatives.

Fig. 2 Residual stress fields τ_{RR} in red and $\tau_{\Theta\Theta}$ in blue showing how the profiles change as higher order radial terms are employed. Here $A = 1, B = 2$ and $\alpha_i = 1$ in all four cases. Panel (a) is for (4.1) and (4.2); panel (b) is for (4.3) and (4.7); panel (c) is for (4.4) and (4.8); panel (d) is for (4.5) and (4.9)

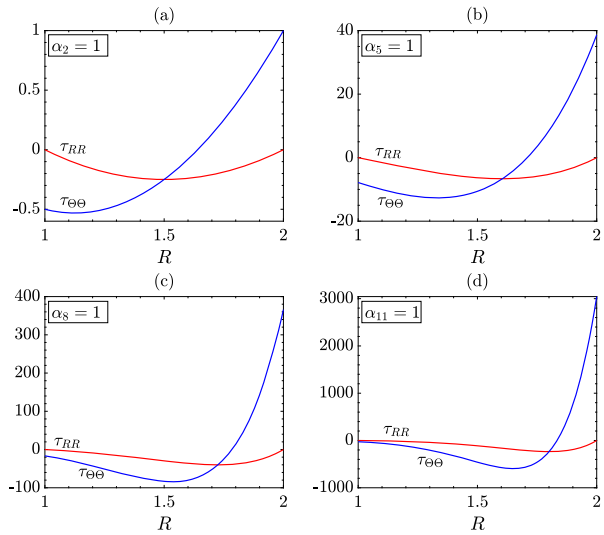
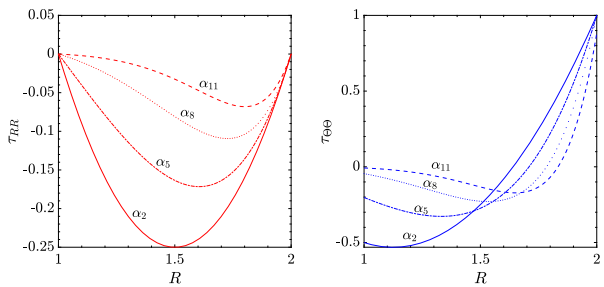


Fig. 3 Stress fields from Fig. 2 with τ_{RR} in the left panel and $\tau_{\Theta\Theta}$ in the right panel, now normalized by taking $\alpha_2 = 1, \alpha_5 = 3/116, \alpha_8 = 31/11344, \alpha_{11} = 225/776192$. This makes $\tau_{\Theta\Theta}(B) = 1$



5 Pressure-Inflation Relations

For a given residually stressed spherical shell, one seeks to determine the relation between the applied load ΔP and the amount of inflation (the value of a in relation to A). For this purpose (3.14) admits to the integration

$$\sigma_{rr}(r) - \sigma_{rr}(a) = \int_a^r 2(\sigma_{\theta\theta} - \sigma_{rr}) \frac{dr}{r}. \tag{5.1}$$

Evaluation of this at $r = b$ using the boundary conditions (3.15) gives

$$\Delta P = \int_a^b 2(\sigma_{\theta\theta} - \sigma_{rr}) \frac{dr}{r}. \tag{5.2}$$

Substituting from (3.12) and (3.13) into the above expression eliminates the hydrostatic pressure p from the treatment. It is further convenient to then decompose the right side of (5.2) as

$$\int_a^b 2(\sigma_{\theta\theta} - \sigma_{rr}) \frac{dr}{r} = P_o + P_\tau, \tag{5.3}$$

where P_o and P_τ gather together the contributions arising from W_o and W_τ , respectively. Consequently

$$\Delta P = P_o + P_\tau \tag{5.4}$$

with

$$P_o = 2\mu \int_a^b \left(\kappa(\lambda^2 - \lambda^{-4}) + (1 - \kappa)(\lambda^4 - \lambda^{-2}) \right) \frac{dr}{r}, \tag{5.5}$$

and

$$P_\tau = 2 \int_a^b \left(\lambda^2 \tau_{\Theta\Theta} - \lambda^{-4} \tau_{RR} \right) \frac{dr}{r}. \tag{5.6}$$

The term P_o is familiar from the conventional hyperelastic theory and readily admits integration using $dr/r = d\lambda/(\lambda - \lambda^4)$. Introduce non-dimensionalized quantities

$$P_o^* = \frac{P_o}{\mu}, \quad \eta = \frac{B}{A}, \quad e = \frac{a^3}{A^3} - 1, \tag{5.7}$$

and note that η serves as an aspect ratio or relative thickness parameter that characterizes the initial shell geometry. The parameter e defines the relative inflation, with $e = 0$ corresponding to the reference state and $e > 0$ corresponding to inflation. The integration of (5.5) now yields

$$P_o^* = \kappa \left(\frac{5\eta^4 + 4e\eta}{2(\eta^3 + e)^{\frac{4}{3}}} - \frac{4e + 5}{2(e + 1)^{\frac{4}{3}}} \right) + (1 - \kappa) \left(\frac{1 + 2e}{(e + 1)^{\frac{2}{3}}} - \frac{\eta^3 + 2e}{\eta(\eta^3 + e)^{\frac{2}{3}}} \right). \tag{5.8}$$

Observe that P_o^* vanishes when $e = 0$, which is consistent with zero pressure in the reference (undeformed) state.

In the absence of residual stress, the inflation relation for hyperelastic spherical shells has been the subject of longstanding study. We close this section with a quick recap of the pressure-inflation response for Mooney-Rivlin spherical shells as given by (5.8). In other words, this recap recalls well known results because it is for the case in which there is no residual stress. The associated pressure-inflation response graphs, with ΔP on the ordinate and either e or a/A on the abscissa, all exhibit an initial inflation, meaning that they all start from $\Delta P = 0$ when $e = 0$ or $a/A = 1$, and all such graphs initially increase with e . However as e continues to increase, one of three behavior types is possible, depending on the values of κ and η . Type (a) behavior is one of continued monotone ΔP increase as $e \rightarrow \infty$. Type (b) behavior involves increase to a local maximum followed by monotone decrease with $\Delta P \rightarrow 0$ in an asymptotic fashion as $e \rightarrow \infty$. Type (c) behavior involves three separate intervals of ΔP response; the first interval involves increase to a local maximum, followed by decrease to a local minimum (with $\Delta P > 0$), and then concluding with monotone graphical increase as $e \rightarrow \infty$.

Type (b) behavior is restricted to the neo-Hookean case ($\kappa = 1$) and this behavior type occurs for all aspect ratios η when the material is neo-Hookean. Type (a) behavior will occur if the Mooney-Rivlin parameter $\kappa < 0.823$ (an exact root expression involving cubics will provide additional precision [5]), and this is again true for all aspect ratios η . For $0.823 < \kappa < 1$, either type (a) or type (c) behavior is possible depending on the aspect ratio η . If the shell is sufficiently thick then type (a) behavior occurs. If it is sufficiently thin then type (c)

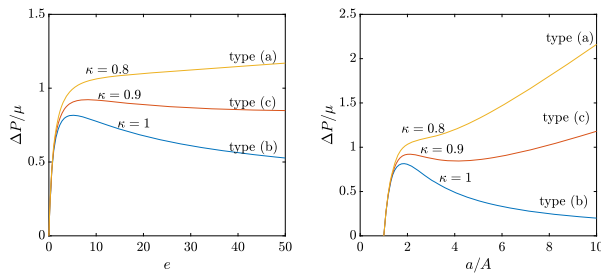


Fig. 4 Mooney-Rivlin material response for a spherical shell with $\eta = B/A = 2$ showing the effect of κ . The neo-Hookean case $\kappa = 1$ gives type (b) behavior. Type (a) response occurs for $0 \leq \kappa < 0.848$ as shown by the $\kappa = 0.8$ response curve. Type (c) response occurs for $0.848 < \kappa < 1$ as shown by the $\kappa = 0.9$ response curve. Left panel shows pressure as a function of e and right panel shows pressure as a function of a/A

behavior occurs. The relation between η and κ that delineates between these two behaviors can be characterized exactly and elegantly, not only for the Mooney-Rivlin material, but also for more general incompressible isotropic hyperelastic materials (in which case additional behavior types are not ruled out [5]).

For our purposes in what follows, we shall continue to provide certain demonstrations using the Mooney-Rivlin base response for a spherical shell with $\eta = B/A = 2$. Then, using the procedure as described in [26], one finds that the transition between type (a) and type (c) behavior occurs for $\eta = 2$ when $\kappa \cong 0.847526$. This is illustrated in Fig. 4 where, for $\eta = 2$, one finds that: $\kappa = 0.8$ gives type (a) behavior, $\kappa = 0.9$ gives type (c) behavior, and $\kappa = 1.0$ gives type (b) behavior.

6 The Residual Stress Integrals

The residual stress effect is governed by the integral for P_τ in (5.6). Because the residual stress fields under consideration occur as linear combinations of powers of R , it is useful to first observe that

$$\bar{\tau}_{RR} = c R^q \quad \Rightarrow \quad \lambda^2 \bar{\tau}_{\Theta\Theta} - \lambda^{-4} \bar{\tau}_{RR} = c (\lambda^2 (1 + \frac{1}{2}q) - \lambda^{-4}) R^q.$$

This motivates the definition

$$P_{\bar{\tau}|q} \equiv \int_a^b ((2 + q)\lambda^2 - 2\lambda^{-4}) R^q \frac{dr}{r}. \tag{6.1}$$

The integral for P_τ in (5.6) will now be expressed in terms of these $P_{\bar{\tau}|q}$. For example, the residual stress field (4.1), (4.2) makes

$$P_\tau = \frac{\alpha_2}{A^2} (P_{\bar{\tau}|2} - (A + B)P_{\bar{\tau}|1} + AB P_{\bar{\tau}|0}). \tag{6.2}$$

6.1 Explicit Integration of $P_{\bar{\tau}|q}$

The explicit integration of $P_{\bar{\tau}|q}$ is complicated by the fact that now R appears in the integrand, along with λ and r . This prompts the introduction of dummy integration variable

$\beta = (\lambda^3 - 1)^{1/3}$ whereupon

$$R = \frac{e^{1/3}A}{\beta}, \quad \lambda = (\beta^3 + 1)^{1/3}, \quad \frac{dr}{r} = -\frac{d\beta}{\beta^4 + \beta}. \tag{6.3}$$

This motivates the additional non-dimensionalized quantity

$$P_{\bar{\tau}|q}^* = \frac{P_{\bar{\tau}|q}}{A^q}. \tag{6.4}$$

One now finds that

$$P_{\bar{\tau}|q}^* = -2e^{\frac{q}{3}} \int_{e^{\frac{1}{3}}}^{e^{\frac{1}{3}/\eta}} \left(\frac{q+2}{2} - \frac{1}{(\beta^3 + 1)^2} \right) \frac{d\beta}{(\beta^3 + 1)^{\frac{1}{3}} \beta^{q+1}}. \tag{6.5}$$

Whether or not (6.5) integrates simply depends upon the value of q . Simple integration, in the sense of not requiring representation in terms of special functions, occurs for $q = 0, 2, 5, 8, \dots 2 + 3n, \dots$. In particular, we find that

$$P_{\bar{\tau}|0}^* = \frac{5 + 4\beta^3}{2(1 + \beta^3)^{\frac{4}{3}}} \Bigg|_{\beta=e^{\frac{1}{3}}}^{\beta=e^{\frac{1}{3}/\eta}}, \tag{6.6}$$

$$P_{\bar{\tau}|2}^* = e^{\frac{2}{3}} \frac{2 - 4\beta^3 - 5\beta^6}{2\beta^2(1 + \beta^3)^{\frac{4}{3}}} \Bigg|_{\beta=e^{\frac{1}{3}}}^{\beta=e^{\frac{1}{3}/\eta}}, \tag{6.7}$$

$$P_{\bar{\tau}|5}^* = e^{\frac{5}{3}} \frac{2 + 5\beta^3 + 16\beta^6 + 12\beta^9}{2\beta^5(1 + \beta^3)^{\frac{4}{3}}} \Bigg|_{\beta=e^{\frac{1}{3}}}^{\beta=e^{\frac{1}{3}/\eta}}, \tag{6.8}$$

$$P_{\bar{\tau}|8}^* = e^{\frac{8}{3}} \frac{10 + 16\beta^3 - 22\beta^6 - 132\beta^9 - 99\beta^{12}}{10\beta^8(1 + \beta^3)^{\frac{4}{3}}} \Bigg|_{\beta=e^{\frac{1}{3}}}^{\beta=e^{\frac{1}{3}/\eta}}, \tag{6.9}$$

and

$$P_{\bar{\tau}|11}^* = e^{\frac{11}{3}} \frac{40 + 55\beta^3 - 28\beta^6 + 126\beta^9 + 756\beta^{12} + 567\beta^{15}}{40\beta^{11}(1 + \beta^3)^{\frac{4}{3}}} \Bigg|_{\beta=e^{\frac{1}{3}}}^{\beta=e^{\frac{1}{3}/\eta}}. \tag{6.10}$$

However other values of q do not lead to such simple expressions. For example $q = 1$ gives

$$P_{\bar{\tau}|1}^* = e^{\frac{1}{3}} \left(\beta^{-1} {}_2F_1 \left[-\frac{1}{3}, \frac{7}{3}, \frac{2}{3}, -\beta^3 \right] - 3\beta^2 {}_2F_1 \left[\frac{2}{3}, \frac{7}{3}, \frac{5}{3}, -\beta^3 \right] - \frac{3}{5}\beta^5 {}_2F_1 \left[\frac{5}{3}, \frac{7}{3}, \frac{8}{3}, -\beta^3 \right] \right) \Bigg|_{\beta=e^{\frac{1}{3}}}^{\beta=e^{\frac{1}{3}/\eta}}, \tag{6.11}$$

where ${}_2F_1[\cdot, \cdot, \cdot, \cdot]$ is the hypergeometric function (see, e.g., [1]) that is defined by the series

$${}_2F_1(a, b, c, z) = \frac{\Gamma(c)}{\Gamma(a)\Gamma(b)} \sum_{n=0}^{\infty} \frac{\Gamma(a+n)\Gamma(b+n)}{\Gamma(c+n)} \frac{z^n}{n!}. \quad (6.12)$$

Here $\Gamma(\cdot)$ is the classical gamma function, which has many formal expressions [19], including

$$\Gamma(\xi) = \int_0^{\infty} t^{\xi-1} e^{-t} dt. \quad (6.13)$$

All of the $P_{\bar{\tau}|q}^*$ as functions of e for $e > 0$ as given by (6.6) - (6.11) are found to take on positive values. Beginning from the initial value $P_{\bar{\tau}|q}^* \Big|_{e=0} = \eta^q - 1$, the graphs are found to increase to a maximum and to then subsequently decrease toward zero as e tends to infinity. This behavior is established in the next subsection.

6.2 Behavior of $P_{\bar{\tau}|q}^*$ for Small and Large e

It is useful to obtain simplified expressions for both the small e and large e behavior of $P_{\bar{\tau}|q}^*$ as functions of the parameters η and q . This is especially true for those q , such as $q = 1$, that do not give straight forward expressions for $P_{\bar{\tau}|q}^*$.

To obtain the small e response we rewrite (6.5) as

$$P_{\bar{\tau}|q}^* = e^{\frac{q}{3}} \int_{e^{\frac{1}{3}}}^{e^{\frac{1}{3}/\eta}} g(q, \beta) \frac{d\beta}{\beta^{q+1}} \quad (6.14)$$

with

$$g(q, \beta) = \frac{1}{(\beta^3 + 1)^{\frac{1}{3}}} \left(-q - 2 + \frac{2}{(\beta^3 + 1)^2} \right). \quad (6.15)$$

Because $g(q, \beta)$ has the small β expansion

$$g(q, \beta) = -q + a_1\beta^3 + a_2\beta^6 + a_3\beta^9 + O(\beta^{12}) \quad (6.16)$$

with

$$a_1 = -4 + \frac{1}{3}q, \quad a_2 = \frac{22}{3} - \frac{2}{9}q, \quad a_3 = \frac{46}{9} + \frac{14}{81}q,$$

it follows from (6.14) that

$$P_{\bar{\tau}|q}^* = e^{q/3} \left(\beta^{-q} + \frac{a_1}{3-q} \beta^{3-q} + \frac{a_2}{6-q} \beta^{6-q} + \frac{a_3}{9-q} \beta^{9-q} + O(\beta^{12-q}) \right) \Bigg|_{\beta=e^{\frac{1}{3}}}^{\beta=e^{\frac{1}{3}/\eta}}, \quad (6.17)$$

provided $q \neq 0, 3, 6, 9$. The cases $q = 0, 3, 6, 9 \dots$ can be considered separately, with $q = 3, 6, 9 \dots$ each yielding up an alternative log term in the above expression.

Finally, evaluating (6.17) between the upper and lower limits now shows that the small e expansion for $P_{\bar{\tau}|q}^*$ begins as

$$P_{\bar{\tau}|q}^* = \eta^q - 1 - \frac{1}{3} \left(\frac{12-q}{3-q} \right) (\eta^{q-3} - 1)e + O(e^2), \quad (6.18)$$

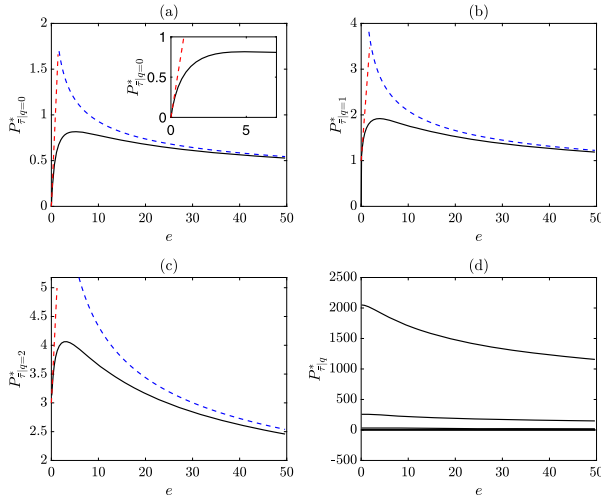


Fig. 5 The solid curves in panels (a) - (c) show the $P_{\bar{\tau}|q}^*$ response graphs as a function of e for $\eta = 2$. Panel (a) is for $q = 0$ as given by (6.6). Panel (b) is for $q = 1$ as given by (6.11). Panel (c) is for $q = 2$ as given by (6.7). The dashed curves in each of these panels depicts the associated small e (red) and large e (blue) response as given by (6.18) and (6.19), respectively. The final panel (d) shows all six graphs $P_{\bar{\tau}|q}^*$ for $q = 0, 1, 2, 5, 8, 11$ on a common plot. Because the initial value $P_{\bar{\tau}|q}^*|_{e=0} = \eta^q - 1 = 2^q - 1$, only the cases $q = 8$ and $q = 11$ are well resolved in the last panel, with the other cases crowded near the e -axis

provided $q \neq 3$ (with $q = 3$ easily treated as its own special case).

For large e consider the large β behavior of $g(q, \beta)$ using (6.15), namely $g(q, \beta) \sim -(q + 2)/\beta$ as $\beta \rightarrow \infty$. This gives

$$P_{\bar{\tau}|q}^* \sim -(q + 2)e^{\frac{q}{3}} \int_{e^{\frac{1}{3}}}^{e^{\frac{1}{3} + \frac{1}{\eta}}} \frac{d\beta}{\beta^{q+2}} = \left(\frac{q + 2}{q + 1}\right) (\eta^{q+1} - 1)e^{-1/3}, \quad \text{as } e \rightarrow \infty. \quad (6.19)$$

The first three panels of Fig. 5 – which consider separately $q = 0, 1, 2$ – provides graphical verification that the small e and large e results give good approximations to the exact integrals on an appropriate range. The final panel of this figure puts all of the graphs for (6.6) - (6.11) on a common plot, so as to also show results for the remaining cases $q = 5, 8, 11$.

6.3 Consequences for P_{τ}

The P_{τ} integral for each of the previously exhibited τ_{RR} fields (4.1), (4.3), (4.4), (4.5) are expressed in terms of the nondimensionalized $P_{\bar{\tau}|q}^*$ as follows:

$$(4.1) \Rightarrow P_{\tau} = \alpha_2 (P_{\bar{\tau}|2}^* - (1 + \eta) P_{\bar{\tau}|1}^* + \eta P_{\bar{\tau}|0}^*), \quad (6.20)$$

$$(4.3) \Rightarrow P_{\tau} = \alpha_5 \left(P_{\bar{\tau}|5}^* - \left(\frac{\eta^5 - 1}{\eta^2 - 1}\right) P_{\bar{\tau}|2}^* + \left(\frac{\eta^2(\eta^3 - 1)}{\eta^2 - 1}\right) P_{\bar{\tau}|0}^* \right), \quad (6.21)$$

$$(4.4) \Rightarrow P_{\tau} = \alpha_8 \left(P_{\bar{\tau}|8}^* - \left(\frac{\eta^8 - 1}{\eta^5 - 1}\right) P_{\bar{\tau}|5}^* + \left(\frac{\eta^5(\eta^3 - 1)}{\eta^5 - 1}\right) P_{\bar{\tau}|0}^* \right), \quad (6.22)$$

$$(4.5) \Rightarrow P_{\tau} = \alpha_{11} \left(P_{\bar{\tau}|11}^* - \left(\frac{\eta^{11} - 1}{\eta^8 - 1}\right) P_{\bar{\tau}|8}^* + \left(\frac{\eta^8(\eta^3 - 1)}{\eta^8 - 1}\right) P_{\bar{\tau}|0}^* \right). \quad (6.23)$$

The coefficients α_i in (6.20) - (6.23) have units of stress. Here it is important to note (see, e.g., Fig. 2) that setting $\alpha_i = 1$ corresponds to very different residual stress field magnitudes for the four cases $i = 1, \dots, 4$. In order to fairly contrast the different fields, we observe that $\tau_{\Theta\Theta}(B)$ is a dominant residual stress value in Fig. 2. This motivates introducing the non-dimensional

$$\alpha_i^* = \tau_{\Theta\Theta}(B)/\mu. \quad (6.24)$$

Consequently, using (4.2), (4.7), (4.8), (4.9), one finds that

$$\alpha_2 = \frac{2}{\eta(\eta-1)}\alpha_2^*\mu, \quad \alpha_5 = \frac{2(\eta^2-1)}{\eta^2(3\eta^5-5\eta^3+2)}\alpha_5^*\mu, \quad (6.25)$$

$$\alpha_8 = \frac{2(\eta^5-1)}{\eta^5(3\eta^8-8\eta^3+5)}\alpha_8^*\mu, \quad \alpha_{11} = \frac{2(\eta^8-1)}{\eta^8(3\eta^{11}-11\eta^3+8)}\alpha_{11}^*\mu. \quad (6.26)$$

The final quantities to nondimensionalize are the P_τ in (6.20) - (6.23). The previous nondimensionalization $P_o^* = P_o/\mu$ from the first of (5.7) motivates

$$P_\tau^* = P_\tau/\mu \quad (6.27)$$

whereupon (5.4) is expressed in the nondimensionalized form

$$\Delta P/\mu = P_o^* + P_\tau^*, \quad (6.28)$$

where P_o^* continues to be given by (5.8). More importantly, P_τ^* in (6.28) now follows from (6.20) - (6.23) in terms of α_i^* . For example,

$$(4.1) \quad \Rightarrow \quad P_\tau^* = \frac{2\alpha_2^*}{\eta(\eta-1)} \left(P_{\bar{\tau}|2}^* - (1+\eta) P_{\bar{\tau}|1}^* + \eta P_{\bar{\tau}|0}^* \right), \quad (6.29)$$

$$(4.3) \quad \Rightarrow \quad P_\tau^* = \frac{2(\eta^2-1)\alpha_5^*}{\eta^2(3\eta^5-5\eta^3+2)} \left(P_{\bar{\tau}|5}^* - \left(\frac{\eta^5-1}{\eta^2-1} \right) P_{\bar{\tau}|2}^* + \left(\frac{\eta^2(\eta^3-1)}{\eta^2-1} \right) P_{\bar{\tau}|0}^* \right). \quad (6.30)$$

Similar style expressions, albeit more complicated ones, follow for P_τ^* upon using (6.26) in the remaining two cases of (6.22) and (6.23). Together this gives four expressions for P_τ^* : one each for (4.1), (4.3), (4.4) and (4.5). Each of these is a function of e on $e > 0$ as determined by the parameters $\eta > 1$ and α_i^* . In each case, and for all parameter values η and α_i^* , one may verify that (6.18) gives that $P_\tau^* = 0$ when $e = 0$.

The advantage of introducing the unit-free coefficient α_i^* is that the various alternative residual stress fields are now expressed in terms of the readily interpretable scaling ratio $\tau_{\Theta\Theta}(B)/\mu$. For $\alpha_i^* > 0$ we find that each of the P_τ^* decreases with e from its initial zero value to a local minimum before again increasing so as to asymptotically give $P_\tau^* \rightarrow 0$ as $e \rightarrow \infty$. The first panel of Fig. 6 shows this behavior for (4.1) and (4.4) on the interval $0 \leq e \leq 25$. The panel shows how this behavior is also reliably predicted upon using the small and large e results for the individual parts $P_{\bar{\tau}|q}^*$ that make up each P_τ^* . The second panel of Fig. 6 confirms that these trends hold also for the remaining two cases by showing P_τ^* on the interval $0 \leq e \leq 40$ for all four cases (4.1), (4.3), (4.4) and (4.5). The new scaling (6.24) now results in the case (4.1) providing the dominant affect for a common value of the dimensionless ratio $\tau_{\Theta\Theta}(B)/\mu$.

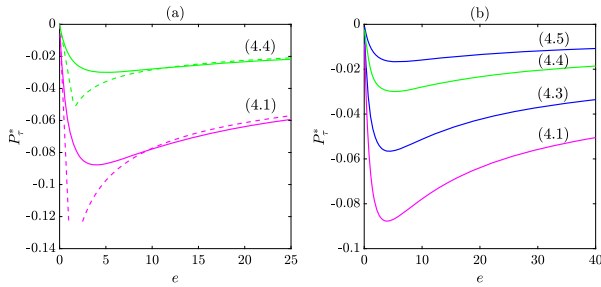


Fig. 6 Behavior of P_τ^* as a function of e for the four cases (4.1), (4.3), (4.4) and (4.5). All graphs are for $\eta = 2$ and $\alpha_i^* = 1$. Panel (a) shows the case (4.1) in purple and the case (4.4) in green. Small and large e approximations are shown in the same color using dashed lines. Panel (b) supplies the remaining graphs for (4.3) and (4.5). The general behavior for $\alpha_i^* > 0$ is monotone decrease to a local minimum followed by asymptotic increase back toward the e -axis. Changing the sign of α_i^* so as to make $\alpha_i^* < 0$ reflects all curves about the horizontal e -axis

7 Effect of Residual Stress on the Pressure-Inflation Relation

The vanishing of P_τ^* both at $e = 0$ and as $e \rightarrow \infty$ indicates that the residual stress effect on the inflation behavior is most consequential for intermediate values of e for the residual stress fields under consideration here. For example, the basic τ_{RR} and $\tau_{\Theta\Theta}$ field pair given by (4.1) and (4.2) generates (6.29) for P_τ^* . If $\alpha_2^* > 0$ then this P_τ^* is negative, with an η dependent value of e that locates its internal minimum. For $\eta = 2$ this internal minimum is at $e \cong 3.9543$. Consequently, it is at this e -value that the residual stress will most affect the inflation graph. Figure 7 exhibits this tendency, where for demonstration purposes the Mooney-Rivlin parameter $\kappa = 0.75$ is employed. The baseline curve for no residual stress is type (a) for $\kappa = 0.75$. As confirmed by the figure, the effect of the residual stress field (4.1), (4.2) on the inflation graph is largest near $e = 4$. Positive values of α_2^* correspond to $\tau_{RR} < 0$ in the shell interior and these lower the inflation graphs. Conversely, interior residual stresses $\tau_{RR} > 0$ raise the graph. This reflects the same tendency for the corresponding 2-D cylindrical geometry problem described in [16]. Similar results follow for the other τ_{RR} fields (4.3), (4.4) and (4.5), although the overall effect is smaller for the same value of $\tau_{\Theta\Theta}(B)$ because of the overall ordering of the various P_τ^* graphs as previously exhibited in Fig. 6.

The specific nature of (2.15), with its separate additive contributions, accounts for the straight forward additive residual stress effect in (6.28) that serves to modify the base response graph (the red curve in Fig. 7). In particular, for $\eta = 2$ and stress field (4.1), (4.2), the residual stress will continue to have its largest effect on the inflation graph near $e = 4$ for other values of the Mooney-Rivlin parameter κ . Indeed, the same holds true if W in (2.15) is modified so as to replace the Mooney-Rivlin form with an alternative base material response.

Staying with the Mooney-Rivlin base response, but considering alternative values of κ , recall from the discussion at the end of Sect. 5 that the value $\kappa \cong 0.847526$ provides the transition between type (a) and type (c) inflation response for $\eta = 2$ when no residual stress is present. The question thus arises as to whether residual stress can alter the type of the inflation response away from its base behavior? The answer to this question is “Yes”. As shown in our final two figures, residual stress can cause a base type (a) response to become type (c), and it can also cause a base type (c) response to become type (a). Technically, such

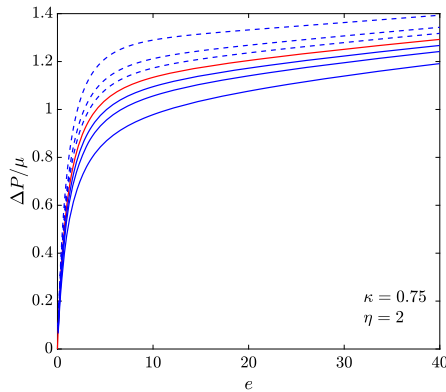
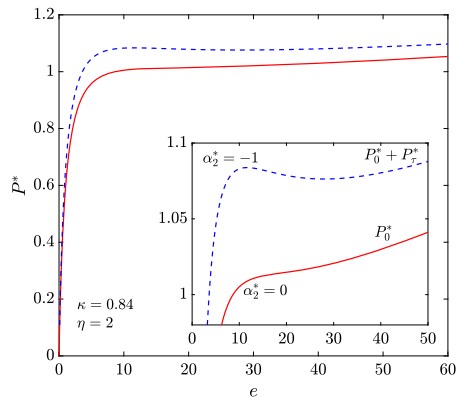


Fig. 7 Inflation graphs as determined by (6.28) for a $\eta = B/A = 2$ spherical shell consisting of a hyperelastic base material described by a $\kappa = 0.75$ Mooney-Rivlin stored energy density W . The residual stress field is given by (4.1) and (4.2). The affect of the residual stress is accounted for in the theory via (2.15) which augments the Mooney-Rivlin energy density with the term $\frac{1}{2}((\text{tr}(\boldsymbol{\tau}\mathbf{C}) - \text{tr}(\boldsymbol{\tau})))$. The central curve in red is the base inflation response ($\alpha_2^* = 0$) corresponding to no residual stress. Solid blue curves correspond progressively to $\alpha_2^* = 0.5, 1, 2$. Dashed blue curves correspond progressively to $\alpha_2^* = -0.5, -1, -2$

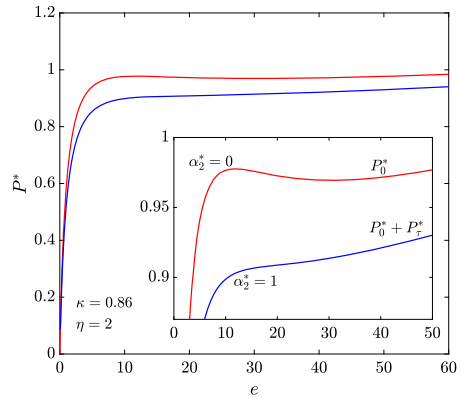
Fig. 8 Type (a) monotonic inflation response occurring for $\eta = 2$ and $\kappa = 0.84$ in the absence of residual stress (red) becomes type (c) nonmonotonic response for the residual stress field pair given by (4.1) and (4.2) with $\alpha_2^* = -1$ (dashed blue)



a result can be made to follow from the decreasing-increasing behavior of P_τ^* for $\alpha_i^* > 0$ and its converse increasing-decreasing behavior for $\alpha_i^* < 0$. Namely, prior to the consideration of residual stress, the transition between type (a) and type (c) behavior is characterized by an inflation graph that is locally flat at some value of e . Specifically, this e locates an inflection point of the base response graph. By contriving to make the inflection point of the base response graph have an e -value that is suitably located with respect to the single extrema of a P_τ^* graph, one can chose α_i^* to push the base response graph into either type (a) or type (c) behavior. More generally, starting with a base response graph that is just to one side of the (a)-to-(c) transition, namely either a definite type (a) response or a definite type (c) response, one can by continuity execute a similar push so as to transition the inflation graph to the other type of response behavior.

To provide a demonstration of a type (a) base response that becomes type (c) for a specific residual stress field, consider $\eta = 2$ and $\kappa = 0.84$. This corresponds to type (a) response in the absence of residual stress (the red curve in Fig. 8). The residual stress field pair given by

Fig. 9 Type (c) nonmonotonic inflation response occurring for $\eta = 2$ and $\kappa = 0.86$ in the absence of residual stress (red) becomes type (a) monotonic response for the residual stress field pair given by (4.1) and (4.2) with $\alpha_2^* = 1$ (blue)



(4.1) and (4.2) with $\alpha_2^* = -1$ is then found to give a type (c) inflation response graph (the dashed blue curve in Fig. 8). Conversely we exhibit a type (c) base response that becomes type (a) for a specific residual stress field by taking $\eta = 2$ and $\kappa = 0.86$. This corresponds to type (c) response in the absence of residual stress (the red curve in Fig. 9). The residual stress field pair given by (4.1) and (4.2) with $\alpha_2^* = 1$ is then found to give a type (a) inflation response graph (the solid blue curve in Fig. 9).

8 Concluding Remarks

The specific additive form $W = W_o + W_\tau$ that is used in this study is motivated by, and in keeping with, prototypical forms that are utilized in previous works. These additive forms are now beginning to see usage in computational treatments (e.g., [8, 22]) that address fundamental questions of bifurcation, imperfection sensitivity and symmetry breaking deformations, all of which are issues that are beyond the scope of this article. In the context of $W = W_o + W_\tau$ we have made use of W_τ given by the first of (2.13). For spherical symmetry this gave rise to integrals (5.6) which had readily determined properties for certain residual stress field expressions. Specifically, a τ_{RR} field that is a linear combination of terms in R^q leads to the consideration of individual integrals given by (6.1). These were then used in the context of W_o given by a Mooney-Rivlin form. The M-R form is of special interest for sphere problems, since it can give either monotone or nonmonotone inflation response as determined by the M-R parameters and the shell thickness. Thus for example it was possible to show how residual stress could potentially cause a nonmonotone response to become monotone, or vice versa, without changing the problem geometry or the constitutive law. Here it is to be noted that the same integrals (6.1) will arise in an alternative treatment that retains $W = W_o + W_\tau$ with W_τ given by the first of (2.13) but with an alternative choice for W_o .

More generally, it is immediate that the form $W = W_o + W_\tau$ with W_τ given by either of (2.13) has the property that the material response reduces to that of a conventional incompressible hyperelastic solid with stored energy W_o in the event that the residual stress τ vanishes. It is important to realize that a separate issue, and one that is not addressed in this paper, is whether or not a given non-vanishing τ could be associated with a specific relaxed configuration that is different from the reference configuration (meaning that there is no residual stress in the relaxed configuration). In other words, whether the hyperelastic

response from the residually stressed reference configuration using $W = W_o + W_\tau$ matches the response from the relaxed configuration using $W = W_o$ or perhaps a suitably modified W_o (meaning a W_o that does not incorporate a residual stress).

Because this issue is not addressed here, care must be taken in describing the meaning of findings encapsulated in, for example, Figs. 8 or 9. That is why our monotone vs. nonmonotone statement in the preceding paragraph avoids describing the results in terms of a residually stressed M-R material. Addressing these types of subtle issues gives rise to broader notions of how to frame such considerations in a fundamental way [11]. Within the specific context of Mooney-Rivlin type response these issues are addressed in [2], where there is a special focus on conditions of plane strain.

Our attention here was also limited to residual stress fields with radial normal stress in the three-term form $\tau_{RR} = k_0 + k_1 R^{q_1} + k_2 R^{q_2}$ for suitably chosen integer exponents $q_2 > q_1 > 0$; these being the simplest nontrivial forms consistent with (3.9). However, such τ_{RR} fields are of one sign, and the resulting $\tau_{\Theta\Theta}$ fields have exactly one internal node. For the purpose of constructing more general residual stress fields that are amenable to the treatment presented here, one may consider the general form containing n terms ($n \geq 3$):

$$\tau_{RR}(R) = \alpha_{3n-4} (c_1 R^0 + c_2 R^2 + c_3 R^5 + \dots + c_{n-1} R^{3n-7} + R^{3n-4}). \quad (8.1)$$

This form, with exponents given in the above particular way, is potentially highly workable for additional analysis because it generates integrals $P_{\tau|q}$ given by (6.1) in terms of specific quotient expressions that do not make use of special functions. Note that the τ_{rr} fields given by (4.3), (4.4) and (4.5) are all special cases of the form (8.1), but (4.1) is not. For example, (4.5) is $n = 5$ with $c_2 = c_3 = 0$ and c_1 and c_4 given by complicated expressions. In general for (8.1), the parameter α_{3n-4} can be regarded as an overall strength-of-field parameter, whereupon the degrees of freedom conferred by the parameters c_1 to c_{n-1} is reduced by two so as to meet the boundary conditions (3.9). Thus the general form (8.1) effectively provides $n-3$ degrees of freedom beyond that of the overall strength-of-field for tuning the form of the residual stress fields.

Acknowledgements This work was sponsored in part by NPRP grant No. 8-2424-1-477 from the Qatar National Research Fund (a member of the Qatar Foundation). The statements made herein are solely the responsibility of the authors.

References

1. Abramowitz, M., Stegun, I.A.: Handbook of Mathematical Functions with Formulas, Graphs, and Mathematical Tables, tenth printing. National Bureau of Standards Applied Mathematics Series, vol. 55 (1972)
2. Agosti, A., Gower, A.L., Ciarletta, P.: The constitutive relations of initially stressed incompressible Mooney-Rivlin materials. *Mech. Res. Commun.* **93**, 4–10 (2018)
3. Beatty, M.F.: Nonlinear effects in fluids and solids. In: Introduction to Nonlinear Elasticity. Mathematical Concepts and Methods in Science and Engineering, vol. 45, pp. 13–112. Plenum Press, New York (1996)
4. Beatty, M.F.: Small amplitude radial oscillations of an incompressible, isotropic elastic spherical shell. *Math. Mech. Solids* **16**, 492–512 (2011)
5. Carroll, M.M.: Pressure maximum behavior inflation of incompressible elastic hollow spheres and cylinders. *Q. Appl. Math.* **45**, 141–154 (1987)
6. Chen, Y.C., Healey, T.J.: Bifurcation to pear-shaped equilibria of pressurized spherical membranes. *Int. J. Non-Linear Mech.* **26**, 279–291 (1991)
7. Chen, Y.C., Hoger, A.: Constitutive functions of elastic materials in finite growth and deformation. *J. Elast.* **59**, 175–193 (2000)
8. Font, A., Jha, N.K., Dehghani, H., Reinoso, J., Meredio, J.: Modeling of residually stressed, extended and inflated cylinders with applications to aneurysms. *Mech. Res. Commun.* **111**, 103643 (2021)

9. Goriely, A.: *The Mathematics and Mechanics of Biological Growth*. Springer, Berlin (2017)
10. Gower, A.L., Ciarletta, P., Destrade, M.: Initial stress symmetry and its application in elasticity. *Proc. R. Soc. Lond. Ser. A* **471**(2183), 20150448 (2015)
11. Gower, A.L., Shearer, T., Ciarletta, P.: A new restriction for initially stressed elastic solids. *Q. J. Mech. Appl. Math.* **40**, 455–478 (2017)
12. Haughton, D.M., Ogden, R.W.: Incremental equations in nonlinear elasticity 2. Bifurcation of pressurized spherical-shells. *J. Mech. Phys. Solids* **26**, 111–138 (1978)
13. Hoger, A.: On the residual stress possible in an elastic body with material symmetry. *Arch. Ration. Mech. Anal.* **88**, 271–290 (1985)
14. Hoger, A.: On the determination of residual stress in an elastic body. *J. Elast.* **16**, 303–324 (1986)
15. Johnson, B.E., Hoger, A.: The dependence of the elasticity tensor on residual stress. *J. Elast.* **33**, 145–165 (1993)
16. Merodio, J., Ogden, R.W.: Extension, inflation and torsion of a residually-stressed circular cylindrical tube. *Contin. Mech. Thermodyn.* **28**, 157–174 (2016)
17. Merodio, J., Ogden, R.W., Rodriguez, J.: The influence of residual stress on finite deformation elastic response. *Int. J. Non-Linear Mech.* **56**, 43–49 (2013)
18. Muller, I., Strehlow, P.: *Rubber and Rubber Balloons: Paradigms for Thermodynamics*. Springer, Berlin (2004)
19. Pence, T.J., Wichman, I.S.: *Essential Mathematics for Engineers and Scientists*. Cambridge University Press, Cambridge (2020)
20. Ricobelli, D., Ciarletta, P.: Shape transitions in a soft incompressible sphere with residual stresses. *Math. Mech. Solids* **23**, 1507–1524 (2018)
21. Rivlin, R.S., Saunders, D.W.: Large elastic deformations of isotropic materials vii: experiments on the deformation of rubber. *Philos. Trans. R. Soc. Lond. A* **243**, 251–288 (1951)
22. Rodriguez, J., Merodio, J.: Helical buckling and postbuckling of pre-stressed cylindrical tubes under finite torsion. *Finite Elem. Anal. Des.* **112**, 1–10 (2016)
23. Shams, M., Ogden, R.W.: On Rayleigh type surface waves in an initially stressed incompressible elastic solid. *IMA J. Appl. Math.* **79**, 360–376 (2014)
24. Shams, M., Destrade, M., Ogden, R.W.: Initial stresses in elastic solids: constitutive laws and acoustoelasticity. *Wave Motion* **48**, 552–567 (2011)
25. Xie, Y.X., Liu, J.C., Fu, Y.B.: Bifurcation of a dielectric elastomer balloon under pressurized inflation and electric actuation. *Int. J. Solids Struct.* **78–79**, 182–188 (2016)
26. Zamani, V., Pence, T.J.: Swelling, inflation, and a swelling-burst instability in hyperelastic spherical shells. *Int. J. Solids Struct.* **125**, 134–149 (2017)
27. Zamani, V., Pence, T.J.: Expansion-contraction behavior of a pressurized porohyperelastic spherical shell due to fluid redistribution in the structure wall. *J. Mech. Mater. Struct.* **15**(1), 159–184 (2020)

Publisher's Note Springer Nature remains neutral with regard to jurisdictional claims in published maps and institutional affiliations.